Molecules and Cells

Enhanced Expression and Functional Characterization of the Recombinant Putative Lysozyme-PMAP36 Fusion Protein

Zhili Rao[1,8], So Young Kim[1,8], Md Rashedunnabi Akanda[2,3], Su Jin Lee[4], In Duk Jung[4], Byung-Yong Park[2], Seralathan Kamala-Kannan[1,5], Jin Hur[6], and Jung Hee Park[1,7,*]

[1]Division of Biotechnology, College of Environmental & Bioresources Sciences, [2]College of Veterinary Medicine and Bio-safety Research Institute, Chonbuk National University, Iksan 54596, Korea, [3]Department of Pharmacology and Toxicology, Sylhet Agricultural University, Sylhet 3100, Bangladesh, [4]Department of Immunology, Laboratory of Dendritic Cell Differentiation and Regulation, School of Medicine, Konkuk University, Chungju 27478, Korea, [5]Advanced Institute of Environment and Bioscience, College of Environmental & Bioresources Sciences, [6]Veterinary Public Health, College of Veterinary Medicine, [7]Safety, Environment and Life Science Institute, College of Environmental and Bioresources Sciences, Chonbuk National University, Iksan 54596, Korea, [8]These authors contributed equally to this work.
*Correspondence: junghee.park@jbnu.ac.kr
http://dx.doi.org/10.14348/molcells.2019.2365
www.molcells.org

The porcine myeloid antimicrobial peptide (PMAP), one of the cathelicidin family members, contains small cationic peptides with amphipathic properties. We used a putative lysozyme originated from the bacteriophage P22 (P22 lysozyme) as a fusion partner, which was connected to the N-terminus of the PMAP36 peptide, to markedly increase the expression levels of recombinant PMAP36. The PMAP36-P22 lysozyme fusion protein with high solubility was produced in *Escherichia coli*. The final purified yield was approximately 1.8 mg/L. The purified PMAP36-P22 lysozyme fusion protein exhibited antimicrobial activity against both Gram-negative and Gram-positive bacteria (*Staphylococcus aureus*, *Salmonella enterica* serovar Typhimurium, *Pseudomonas aeruginosa*, and *Bacillus subtilis*). Furthermore, we estimated its hemolytic activity against pig erythrocytes as 6% at the high concentration (128 μM) of the PMAP36-P22 lysozyme fusion protein. Compared with the PMAP36 peptide (12%), our fusion protein exhibited half of the hemolytic activity. Overall, our recombinant PMAP36-P22 lysozyme fusion protein sustained the antimicrobial activity with the lower hemolytic activity associated with the synthetic PMAP36 peptide. This study suggests that the PMAP36-P22 lysozyme fusion system could be a crucial addition to the plethora of novel antimicrobials.

Keywords: circular dichroism spectroscopy, hemolytic activity, minimum inhibitory concentration, porcine myeloid antimicrobial peptide, transmission electron microscope

INTRODUCTION

Globally, drug-resistant clinical pathogens have become a major problem (Jacoby et al., 2010). Hence, various kinds of antimicrobial peptides (AMPs) have been considered as antimicrobial candidates clinically. AMPs, known as host defense peptides, have been reported from various organisms (Zasloff, 2002); they have broad activity spectra against bacterial pathogens, as well as virus, fungi, and even other parasites (Hancock and Sahl, 2006; Lv et al., 2014). The Antimicrobial Peptide Database lists almost 3000 AMPs from six kingdoms (Wang et al., 2016). Contrary to common antibiotics with an inhibitory effect on biosynthetic pathways,

Received 1 September, 2018; revised 24 December, 2018; accepted 27 January, 2019; published online 19 February, 2019

eISSN: 0219-1032

AMPs activity has been recognized on microbial cell membranes (Teixeira et al., 2012). Although the precise mechanism of AMPs remains unclear, the interaction of AMPs is believed to increase the permeability or inhibit the barrier function of the host membrane by forming pores (Mai et al., 2015; Teixeira et al., 2012). Mammalian AMPs are known as major components of the innate and adaptive immune systems and to be involved in the direct destruction of bacteria (Yeung et al., 2011).

Typically, AMPs can be classified in numerous ways such as properties of peptides, functions, structures, etc.; Of these, cationic AMPs are derived from larger precursors through proteolysis or a kind of chemical modifications (Bulet et al., 1993; Subbalakshmi et al., 2000; Tang et al., 1999; van Kan et al., 2003; Zasloff, 2002; Zheng et al., 2007). The secondary structure of mature AMPs comprises four major groups as follows: (1) amphipathic α-helices; (2) β-sheet peptides stabilized by disulfide bonds; (3) extended helix structures rich in specific amino acids like indolicidin; and (4) irregular peptide structure, such as actenecin (Hancock and Sahl, 2006; Huang et al., 2010; Yeaman and Yount, 2003). The structural features of cationic AMPs frequently display a relatively short length of <50 residues, high net positive charge, and a substantial proportion of nonpolar amino acids (Bahnsen et al., 2015; Hancock and Sahl, 2006). Interestingly, the secondary structure of amphipathic α-helices cationic AMPs deviates from disordered coil form in the aqueous state to amphipathic α-helical conformation in hydrophobic or membrane-mimicking environments (Li et al., 2012; Takahashi et al., 2010). The deviation into amphipathic α-helical conformation is crucial for attaining the highest antimicrobial effect; the AMPs with β-sheet and random coils exhibit a relatively low or no antimicrobial activity (Mai et al., 2015).

Porcine myeloid antimicrobial peptides (PMAPs), as the name suggests, are derived from the myeloid cells of pigs; PMAP23, PMAP36, and PMAP37 are the most common PMAPs, which belong to the cathelicidin family members that have a C-terminal cationic antimicrobial domain (Scocchi et al., 2005; Storici et al., 1994). One of the PMAPs, PMAP36 protein, comprises a 29-amino acid signal peptide in the N-terminus, a 101-amino acid prosequence, and 36-amino acid peptide from the C-terminus (GRFRRLRKKTRKRL KKIGKVLKWIPPIVGSIPLGCG). Reportedly, the PMAP36 peptide is highly cationic owing to the 36% cationic amino acids (Lv et al., 2014; Storici et al., 1994). Although it exhibits antimicrobial properties, it displays high toxicity because of hemolysis (Lv et al., 2014; Lyu et al., 2016; Scocchi et al., 2005). Hence, as an antimicrobial agent, the chemically synthesized PMAP36 peptide is not suitable. Thus, attempts to increase its antimicrobial effect and degrade its toxicity have been made using analogs of the PMAP36 peptide (Lv et al., 2014; Lyu et al., 2016; Scocchi et al., 2005; Storici et al., 1994). Although a precise killing mechanism of the PMAP36 peptide remains unclear to date, it is usually anticipated to exert a common lytic action; this anticipation has been supported by circular dichroism (CD) spectra. Using a structural approach based on the results obtained from CD spectra, some previous studies have reported a peptide-lipid-induced conformational change of the PMAP36 peptide from a random coil in aqueous buffer to α-helical conformation in membrane-mimic environments (Lyu et al., 2016; Storici et al., 1994).

The recombinant protein expression was usually performed on heterologous microbial expression systems to obtain a sufficient quantity of AMPs (Ingham and Moore, 2007). In addition, for successful recombinant protein expression, several factors, such as an appropriate vector system, codon usage, host cells, the signal peptide, and a fusion partner, should be considered. Fusion partners are used to amplifying the protein expression level and protein stability. In this study, we selected the lysozyme originated from the bacteriophage P22 as a fusion partner. The bacteriophage P22 was discovered from *Salmonella enterica* serovar Typhimurium, and the whole genome sequence of 28 fragments was resolved (Pedulla et al., 2003). In host cells, P22 lysozyme encoded from gene 19 of the bacteriophage P22 exhibits lytic activity (Rennell and Poteete, 1989). This study aims to report the overexpression, purification, and characterization of the recombinant PMAP36 peptide connected with a fusion partner P22 lysozyme, called PMAP36-P22 lysozyme fusion protein, which can increase the production of the soluble PMAP36 peptide. The PMAP36-P22 lysozyme fusion protein displays low toxicity and possesses antimicrobial activity against Gram-positive and Gram-negative bacteria.

MATERIALS AND METHODS

Construction of the recombinant PMAP36-P22 lysozyme fusion protein plasmid

The genes of lysozyme from the bacteriophage P22 (P22 lysozyme; GenBank accession no. AAM81442) and PMAP36 peptide (GenBank accession no. NP001123437) were chemically synthesized with codon optimization based on *Escherichia coli* codon preferences (Bioneer, Korea). Using polymerase chain reaction (PCR), each gene was amplified with a primer set (Table 1). The thrombin cleavage site was added

Table 1. Primer sets for cloning PMAP36-P22 lysozyme fusion protein

Primer name	Sequence (5'-3')
P22 lyso forward	CATATGCACCATCATCACCATCACATGCAAATCAGCAGTAACGG
P22 lyso reverse	GGATCCACGCGGAACCAGCGATAAGAACAGCGCTCTTTC
PMAP36 forward	GGATCCGGACGATTTAGACGTTTACG
PMAP36 reverse	GCGGCCGCTTATCCACAACCTAAGGGTATTGAAC

with PCR at the C-terminus of P22 lysozyme. In more details, the amplified P22 lysozyme gene and pET30a vector were digested with restriction enzymes, *Nde*I and *Bam*HI, and ligated. Then, the amplified *PMAP36* gene was inserted into the recombinant plasmid pET30a-P22 lysozyme by *Bam*HI and *Not*I restriction site. After that, the recombinant plasmid pET30a-P22 lysozyme-PMAP36 (PMAP36-P22 lysozyme fusion protein) was transformed to the *E. coli* DH5α cells.

Expression and purification of the PMAP36-P22 lysozyme fusion protein

The recombinant plasmid pET30a-P22 lysozyme-PMAP36 was transformed in *E. coli* BL21 (DE3) for fusion protein expression. For large-scale expression, we inoculated a single colony into 100 mL Luria-Bertani (LB) broth containing 50 μg/ml kanamycin and incubated at 37℃ and 200 rpm for overnight. Next, 10 ml of seed culture was transferred to 1 L LB broth containing 50 μg/ml kanamycin in a baffled flask; the culture was grown at 37℃ and 200 rpm until OD_{600} was 0.6. We induced the recombinant protein expression by adding 0.5 mM isopropyl-b-D-thiogalactopyranoside (IPTG) and incubated the cells for 24 h at 28℃ and 170 rpm. The cultured cells were harvested by high-speed centrifugation at 1400 × *g* for 15 min at 4℃. On the other hand, we investigated the growth behavior of *E. coli*, including the PMAP-P22 lysozyme fusion protein plasmid, during the expression culture (Supplementary method).

For purification, the harvested cells were resuspended in 20 ml lysis buffer (10 mM Tris-HCl, pH 8.0, 1 M NaCl) and lysed by pulsed sonication (Sonic) of 4-s sonic and 4-s rest on ice. We collected the soluble protein lysate by high-speed centrifugation at 16,000 × *g* for 25 min at 4℃. The supernatant was filtered by a syringe filter (0.45 μm) and loaded into the HisTrap FF column connected in the ÄKTA prime FPLC system (GE Healthcare). The column was washed by lysis buffer, which we used as buffer A. The protein samples were eluted by a linear gradient with buffer B (10 mM Tris-HCl, pH 8.0, 1 M NaCl, 300 mM imidazole). Each elution fraction was analyzed by 15% SDS-PAGE. The purified PMAP36-P22 lysozyme fusion protein was dialyzed with buffer C (PBS buffer; GE Healthcare) and concentrated by Centricon (cutoff 10 kDa; Amicon, Germany). Finally, we determined the concentration of the PMAP36-P22 lysozyme fusion protein using the Bradford protein assay (Bio-Rad).

Western blotting

We analyzed the purified and concentrated PMAP36 fusion protein by 15% SDS-PAGE. After transferring the protein to the PVDF membrane (Millipore), we used anti-6-his polyclonal antibody (BD, France) and HRP-conjugated goat anti-mouse IgG antibody (Enzo) as a primary antibody (1:6,000 dilution) and secondary antibody (1:12,000 dilution), respectively. The protein band was visualized with the ECL solution (SurModics).

CD spectroscopy

We monitored the purified PMAP36-P22 lysozyme fusion protein using far-UV CD spectroscopy (JASCO J-1500 spectropolarimeter, wavelength range: 190-260 nm) to evaluate the secondary structure and folding properties. The spectra were measured for each sample of 0.5 mg/ml (P22 lysozyme, PMAP36 peptide, and PMAP36-P22 lysozyme fusion protein) in buffer D (PBS buffer (GE Healthcare) containing 50% glycerol (*v*/*v*)) and buffer D including 1% SDS, respectively, at 25℃ using a quartz cuvette of 0.1-cm path length. For data collection, we recorded the spectrum for each sample with an average of three scans using a scan speed of 200 nm/min, bandwidth of 1.0 nm, and response time of 1 s.

Antimicrobial assay

We determined the minimal inhibitory concentration (MIC) of the fusion protein, as described previously (Lv et al., 2014), using *Staphylococcus aureus*, *S. enterica* serovar Typhimurium, *Pseudomonas aeruginosa*, and *Bacillus subtilis*. Next, overnight cultured microbes were diluted to 1×10^5 CFU/ml, mixed with P22 lysozyme, PMAP36 peptide, and PMAP36-P22 lysozyme fusion protein (final concentration: 0.125-128 μM), and incubated at 37℃ for 24 h. Then, 10 μl mixture was dropped on Mueller-Hinton (MH) agar plate and incubated at 37℃ for 18 h. The MIC results were interpreted by colony formation. In addition, we used four different antibiotics as references (final concentration: 0.125-128 μg/ml) to check the antibiotics sensitivity as described above (Supplementary Table 2).

The reaction with P22 lysozyme without PMAP36 was performed as a negative control. MH broth (BD) without cells and cultures without protein were used as negative and positive control, respectively.

Transmission electron microscope

We performed transmission electron microscope (TEM) analysis according to the established protocol (Lv et al., 2014). Briefly, samples were prepared after an experimental treatment procedure; the samples were washed three times with PBS by centrifugation at 5000 × *g* for 5 min. The bacterial pellets were fixed with 2.5% glutaraldehyde in 0.2 M cacodylate buffer for overnight at 4℃ and washed three times with PBS. In addition, 1% osmium tetroxide in 0.2 M cacodylate buffer was used for post-fixing for 2 h. After three-time washing with PBS, the fixed samples were dehydrated in a graded series of ethanol (50%, 70%, 90%, 95%, and 100%) for 20 min, respectively. We placed dehydrated samples in absolute propylene oxide for 30 min and sequentially transferred to 1:1 and 1:3 mixture of absolute propylene oxide and epoxy resin for 1.5 h, respectively. Finally, the samples were transferred to the pure epoxy resin for overnight at 37℃. After that, samples were sliced using ultramicrotome, post-stained with uranyl acetate and lead citrate, and examined by TEM (Hitachi H-7650, Japan).

Outer membrane permeabilization activity

We determined the activity of outer membrane permeabilization by ethidium bromide (EtBr) influx assay as described previously (Miki and Hardt, 2013). The cell cultures at mid-logarithmic phase, OD_{600} of 0.2, were mixed with PBS (GE Healthcare) and PMAP36-P22 lysozyme fusion protein (final concentration: 64 μM) and incubated for 10 min at 37℃. We added EtBr (final concentration: 6 μM) to the reaction mix-

ture and measured the fluorescence using fluorescence spectrometer (Infinite 200® Pro, TECAN, Austria); the excitation and emission wavelengths were 545 and 600 nm, respectively.

Hemolytic assay

We performed the hemolytic assay by measuring the amount of released hemoglobin from the pig erythrocytes as described previously (Lv et al., 2014). In addition, we measured the hemolytic activity of P22 lysozyme to compare with the PMAP36-P22 lysozyme fusion protein activity. PBS (GE Healthcare) and 0.1% Triton X-100 in PBS (*v*/*v*) were used as the negative and positive control, respectively.

Generation and culture of bone marrow-derived dendritic cells

We extracted tibias and femurs from 6-week-old female C57BL/6 mice and flushed out the bone marrow; this preparation was depleted of red blood cells (RBCs) by treatment with an RBC-lysing buffer (Sigma-Aldrich). Bone marrow-derived dendritic cells (BMDCs) were then seeded onto 6-well culture plates (1×10^6 cells/ml; 2 ml/well) in RPMI-1640 supplemented with 10% heat-inactivated fetal bovine serum, 100 U/ml penicillin, 100 mg/ml streptomycin, and 10 ng/ml rmGM-CSF at 37℃ under an atmosphere containing 5% CO_2. On days 3 and 5, nonadherent cells were carefully removed, and fresh medium was added. On day 6, we harvested all nonadherent cells, loosely adherent, and proliferating DC aggregates for analysis or LPS stimulation. On day 7, we found that ≥ 90% of nonadherent cells expressed CD11c (data not shown).

Cytokine enzyme-linked immunosorbent assays

We determined the quantities of TNF-α, IL-1β, IL-6, IL-10, and IL-12p70 in the culture supernatants and mouse sera using sandwich enzyme-linked immunosorbent assays kits (eBioscience), per the manufacturer's instructions (Ding et al., 2017).

RESULTS AND DISCUSSION

Expression and purification of the PMAP36-P22 lysozyme fusion protein

In this study, we selected the lysozyme originated from the bacteriophage P22 as a fusion partner and N-terminus of the PMAP36 peptide was connected with C-terminus of P22 lysozyme (PMAP36-P22 lysozyme fusion protein; Fig. 1).

Occasionally, proteins with antimicrobial activity could account for inhibiting bacterial growth during expression. We used two different bacteria, *E. coli* including vehicle (negative control) and *E. coli* transformed by recombinant plasmid pET30a-P22 lysozyme-PMAP36 (PMAP36-P22 lysozyme fusion protein) in cell growth and expression to investigate the inhibitory effect of the growth of *E. coli* including the PMAP36-P22 lysozyme fusion protein. Compared with the negative control, the cell growth of the PMAP36-P22 lysozyme fusion protein-expressed *E. coli* exhibited no significant difference (Supplementary Fig. 1), suggesting that the PMAP36-P22 lysozyme fusion protein has no inhibitory effect on the cell growth.

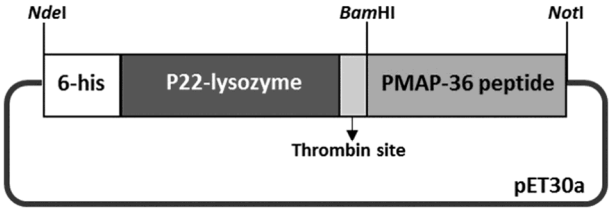

Fig. 1. The construct of recombinant plasmid encoded PMAP36-P22 lysozyme fusion protein.

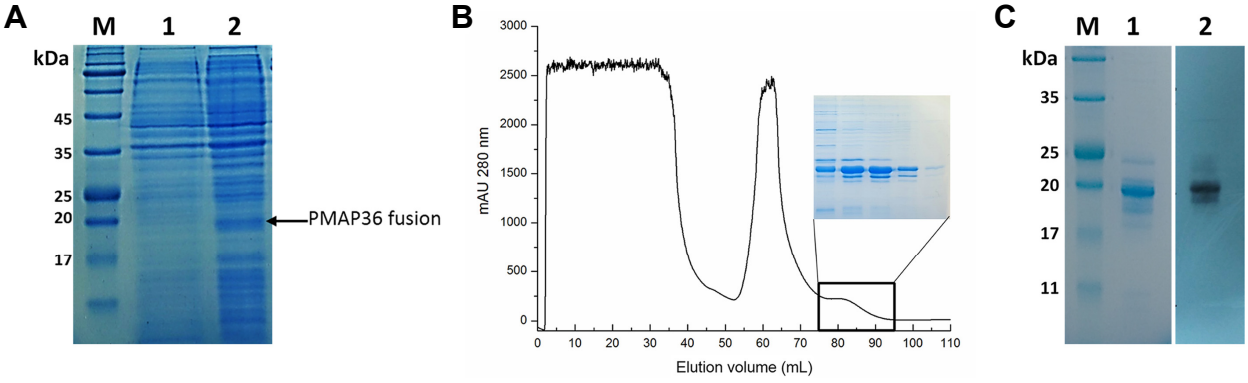

Fig. 2. Expression and purification of PMAP36-P22 lysozyme fusion protein. (A) The expression of fusion protein was detected using 15% SDS-PAGE gel. The fusion protein overexpression was induced by 0.5 mM IPTG at 28℃ for 24 h in *E. coli* BL21 (DE3). The PMAP36-P22 lysozyme fusion protein band was shown at a little lower than 20 kDa. (M: size marker, lane 1: whole lysate before induction, lane 2: whole lysate after induction) (B) The chromatogram during the purification of PMAP36-P22 lysozyme fusion protein using the ÄKTA Prime FPLC system and Histrap FF column. (Inset: The eluted fractions were confirmed with 15% SDS-PAGE) (C) The finally purified and concentrated PMAP36-P22 lysozyme fusion protein was confirmed by 15% SDS-PAGE (lane 1) and western blotting (lane 2). 2.5 μg of protein was loaded in the well.

To obtain high expression levels of the recombinant PMAP36-P22 lysozyme fusion protein, it was overexpressed in *E. coli* and analyzed by 15% SDS-PAGE (Fig. 2A). For the highest expression level of the recombinant PMAP36-P22 lysozyme fusion protein, the optimized condition was investigated by alterations of temperature, aeration speed, concentration of IPTG, and protein expression time. In addition, the increased solubility of the fusion protein was obtained at 28℃, 170 rpm (final concentration: 0.5 mM IPTG).

The expressed PMAP36-P22 lysozyme fusion protein contains 6-histidine tag at N-terminus and, hence, was purified using affinity chromatography, Ni^{2+}-NTA affinity column. Figure 2B presents the elution profile of the PMAP36-P22 lysozyme fusion protein in affinity chromatography using the Ni^{2+}-NTA affinity column. The eluted fractions containing the PMAP36 fusion proteins were analyzed for purity using SDS-PAGE (Fig. 2B, inset). Finally, the purified PMAP36 fusion protein was concentrated to >10 mg/ml, and the purified protein was confirmed by SDS-PAGE and western blotting, respectively (Fig. 2C). The final yield of the purified protein was 1.8 mg/1 L culture, and the purity was approximately 80%. To approach practical applications of the antimicrobial industry, our study will be furthered to improve its productivity.

The secondary structure of the PMAP36-P22 lysozyme fusion protein from CD spectroscopy

We used far-UV CD spectroscopy to investigate the comparison of the secondary structure with the PMAP36-P22 lysozyme fusion protein, as well as P22 lysozyme and PMAP36 peptide (Fig. 3). The CD spectrum of α-helical structure typically suggests two negative bands at 208 and 222 nm. We estimated the helical contents of three different samples with molar ellipticity and a degree of helicity. In the aqueous phase, the spectrum of the PMAP36 peptide predominantly exhibited random coil conformation, consistent with predictions of the secondary structure in a previous study (Lv et al., 2014). On the other hand, in P22 lysozyme and PMAP36-P22 lysozyme fusion protein, these spectra in the same phase exhibited a similar secondary structure with α-helical contents of 21.6% and 17.3%, respectively (Fig. 3A). The α-helical contents of the PMAP36-P22 lysozyme fusion protein are slightly lower than that of P22 lysozyme. The reduction of α-helical contents of the PMAP36-P22 lysozyme fusion protein compared with that of P22 lysozyme could be attributed to the random coil contents of the PMAP36 peptide, suggesting no significant changes in the PMAP36 peptide in the fusion protein.

In the membrane-like phase (1% SDS in buffer D), the α-helical contents of the PMAP36-P22 lysozyme fusion protein (26.70%) were significantly increased compared with that in the aqueous phase (Fig. 3B). In addition, the increased α-helical contents of the PMAP36 peptide (38.80%) were dramatically observed, as reported previously (Lv et al., 2014). These results suggested that a change in secondary structures of the PMAP36-P22 lysozyme fusion protein and PMAP36 peptide correlates with enhanced α-helical contents in the membrane-like phase. Furthermore, the increased α-helical content of the PMAP36-P22 lysozyme fusion protein and the PMAP36 peptide could be crucial for the bacterial activity as reported previously (Li et al., 2012; Takahashi et al., 2010).

Antimicrobial activity of the PMAP36-P22 lysozyme fusion protein

Although the secondary structure of the PMAP36 peptide from the PMAP36-P22 lysozyme fusion protein was estimated as a random coil, the antimicrobial activity of the PMAP36-P22 lysozyme fusion protein was monitored for its broad range of activity against Gram-negative (*S.* Typhimurium and *P. aeruginosa*) and Gram-positive (*B. subtilis* and *S. aureus*) microorganisms. Table 2 presents the MIC for Gram-negative and Gram-positive bacteria. We determined the MIC value of the PMAP36-P22 lysozyme fusion protein and compared it with that of P22 lysozyme and PMAP36 peptide.

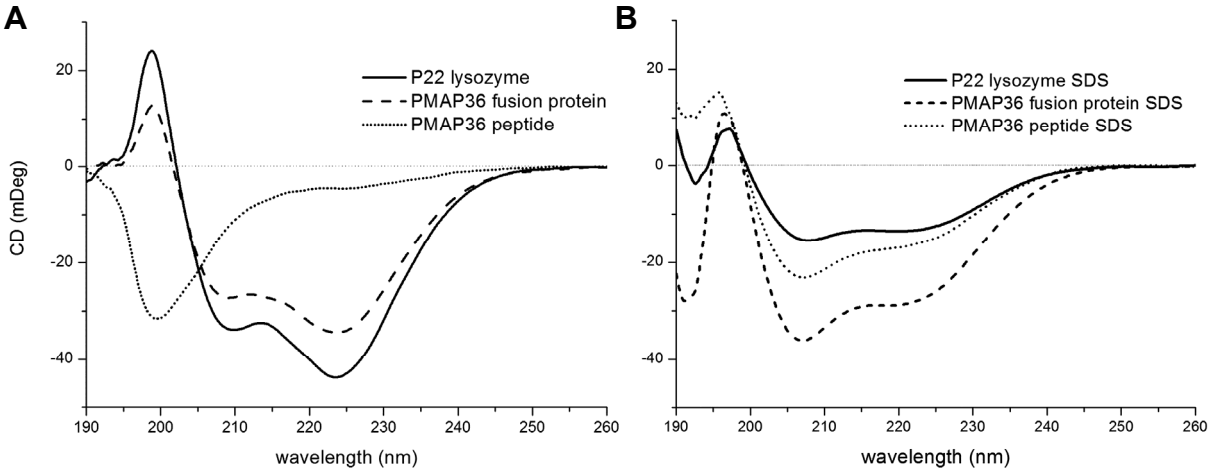

Fig. 3. Secondary structure CD spectra of the P22 lysozyme (straight line), PMAP36-P22 lysozyme fusion protein (dash) and PMAP36 peptide (dot) in PBS (A) and 1% SDS (B). The concentration of all proteins and peptide were 0.5 mg/ml.

Table 2. Antimicrobial activity of P22 lysozyme, PMAP36-P22 lysozyme fusion protein and PMAP36 peptide against 4 different microorganisms. Minimal inhibitory concentrations (MICs) were defined as the lowest concentration (μM) of both proteins which inhibit the cell growth

	P22 lysozyme	PMAP36 fusion	PMAP36 peptide
B. Subtilis	1	<0.25	2
S. Aureus	>128	8	8
P. Aerusinosa	>128	16	8
S. Typhimurium	>128	2	4

The antimicrobial activity of the PMAP36-P22 lysozyme fusion protein was 4-64 times higher than that of P22 lysozyme (Table 2). In addition, the MICs of the PMAP36-P22 lysozyme fusion protein against tested microorganisms, except *B. subtilis*, indicated the range to be 2-16 μM, which was similar to that of the synthetic PMAP36 peptide. Of note, the MIC results of microbes with the PMAP36 peptide in the four tested bacteria was higher than that reported previously (Lv et al., 2014), suggesting that this reason is probably attributed to the specificity of other strains. Consequently, our findings revealed that P22 lysozyme as a fusion partner might not affect the antimicrobial activity of the PMAP36 peptide.

We evaluated the TEM analysis to observe the ultrastructural membrane integrity and intracellular change of bacterial cells before and after treatment with the PMAP36-P22 lysozyme fusion protein to investigate an effect of the PMAP36-P22 lysozyme fusion protein on the cell morphology. Among cells used in the MIC analysis, *B. subtilis* was excluded because it was not cultured with the PMAP36-P22 lysozyme fusion protein. The TEM image of untreated control bacterial cells revealed a normal cell shape with an undamaged, complete architecture of the inner membrane and marginally waved outer membrane (Fig. 4). Furthermore, the periplasmic area was thin and had a homogeneous cytoplasm. Conversely, the PMAP36-P22 lysozyme fusion protein treatment induced marked rupture of the cell membrane, the release of intracellular contents, and evident cytoplasmic clear zone. The cytoplasmic membrane of cells was observed as irregular and detached from the outer cell membrane. Overall, the PMAP36-P22 lysozyme fusion protein worked both Gram-positive and Gram-negative cells differently. In the case of Gram-positive cells (*S. aureus*), the cell membrane completely disappeared post-treatment instead of making a hole in the membrane (Fig. 4).

Outer membrane permeabilization, hemolytic activity, and immunomodulatory effect of the PMAP36-P22 lysozyme fusion protein

The ability of outer membrane penetration was investigated by the EtBr influx assay to investigate the antimicrobial effect of the PMAP36-P22 lysozyme fusion protein in the cell membrane (Fig. 5A). When EtBr binds to the intracellular DNA, the highly enhanced fluorescence can be monitored using a fluorescence spectrophotometer. However, the intact outer membrane barrier prevents the translocation of EtBr into the cytoplasm (Miki and Hardt, 2013). In this assay, we used PBS buffer as the negative control and monitored the fluorescence signal for outer membrane penetration. Of note, the intensities of fluorescence signal were enhanced in the PMAP36-P22 lysozyme fusion protein-treated microorganisms irrespective of the species. In all experimental microorganisms, the fluorescence signal was increased by about two to three times relative to the PBS buffer. The increase in fluorescence intensities suggests that the activity of the PMAP36-P22 lysozyme fusion protein damages the bacterial membrane. Our findings, thus, revealed that the PMAP36-P22 lysozyme fusion protein is a potent antimicrobial agent.

To date, the high toxicity of the synthetic PMAP36 peptide has been reported as the major drawback, and trials for minimizing the PMAP36 toxicity were conducted using mutagenesis studies such as site-directed mutants or truncated mutants (Lv et al., 2014; Lyu et al., 2016). Accordingly, we measured the hemolytic activity of the PMAP36-P22 lysozyme fusion protein and PMAP36 peptide using pig erythrocytes to investigate the toxicity of the PMAP36-P22 lysozyme fusion protein against mammalian cells (Fig. 5B). Our findings revealed that the hemolytic activity of the PMAP36-P22 lysozyme fusion protein was marginally observed in a concentration-dependent manner, whereas the hemolytic activity of the PMAP36 peptide was observed (Fig. 5B). The relative

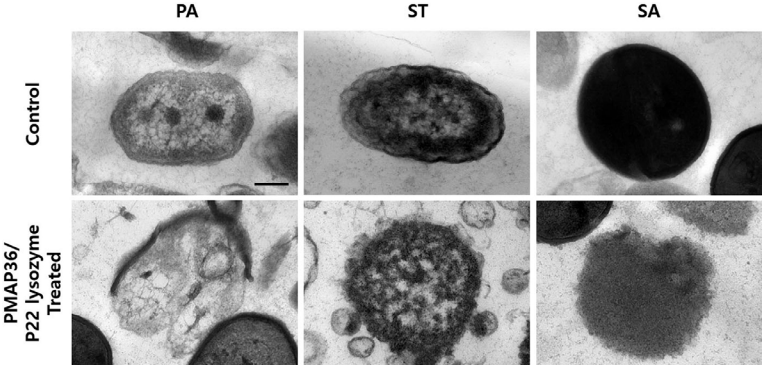

Fig. 4. TEM images of bacterial cells treated with PMAP36-P22 lysozyme fusion protein. The bacteria cells were incubated in the presence or absence of the PMAP36-P22 lysozyme fusion protein at MIC for 60 min at 37℃. The scale bar in the upper left panel represents 0.2 um (PA: *P. aeruginosa*, ST: *S.* Typhimurium, SA: *S. aureus*)

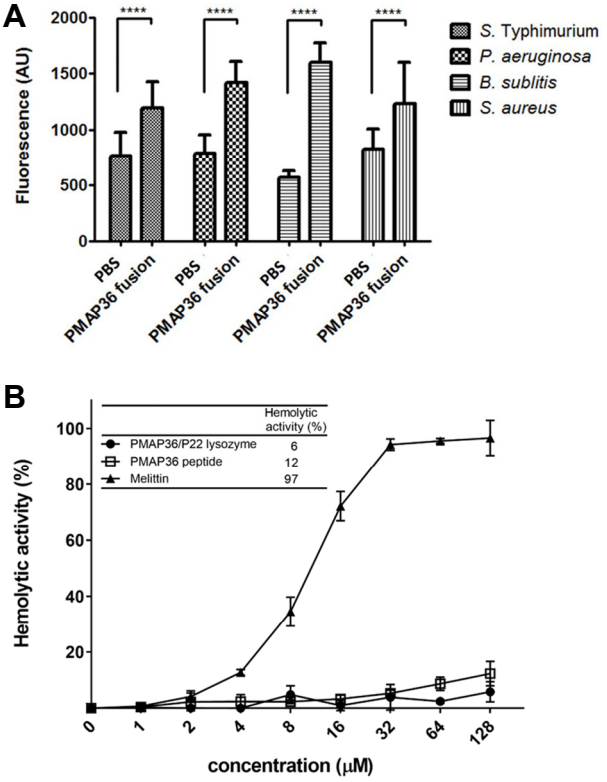

Fig. 5. Antimicrobial activities. (A) Outer membrane permeability of 4 kinds of microbe (2 Gram-negative and 2 Gram-positive bacteria) was measured using PMAP36-P22 lysozyme fusion protein by EtBr influx assay. The activities were compared with PBS buffer as a control. The error bars show the standard deviation of the mean from three independent trials. Asterisks indicate statistically significant differences between groups. (****, Unpaired *t*-test, $P < 0.0001$) (B) Concentration dependent hemolytic activities of PMAP36-P22 lysozyme fusion protein and PMAP36 peptide. After treatment of proteins against pig erythrocytes, the absorbance of releasing hemoglobin was measured at 570 nm. Data were calculated from three independent trials. (Inset: The relative hemolytic activity of PMAP36-P22 lysozyme fusion protein, PMAP36 peptide and melittin at the highest concentration (128 μM)).

hemolytic activity was detected in approximately 6% of the PMAP36-P22 lysozyme fusion protein and 12% of the PMAP36 peptide at the highest concentration (at 128 μM) compared with the hemolytic activity of detergent-treated pig erythrocytes (Fig. 5B, inset). Unlike previously reported mutagenesis studies (Lv et al., 2014), the PMAP36-P22 lysozyme fusion system, without any modification of the antibacterial region, was used to retain the antimicrobial activity and have lower hemolytic activity than that of the synthetic PMAP36 peptide.

To test the effect of immunogenic response with the PMAP36-P22 lysozyme fusion protein and P22 lysozyme in BMDCs, the levels of inflammatory cytokines, such as TNF-α, IL-1β, IL-6, IL-10, and IL-12p70, in BMDCs after stimulation

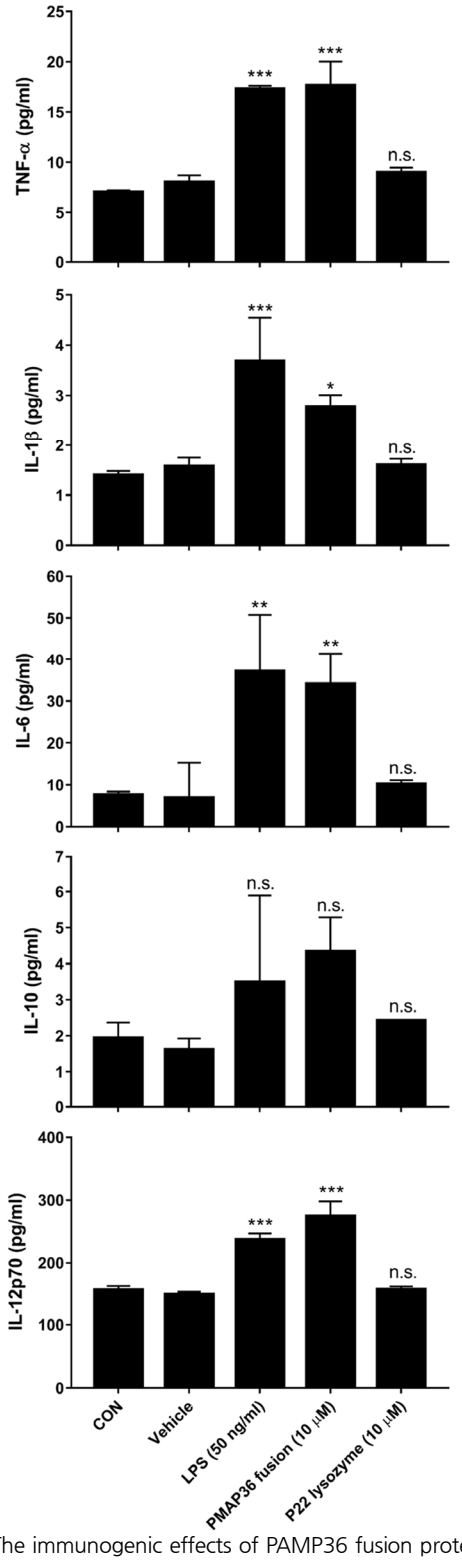

Fig. 6. The immunogenic effects of PAMP36 fusion protein and P22 lysozyme in DCs. DCs were treated with PAMP36 (10 μg/ml), P22 (10 μg/ml) or LPS (50 ng/ml) and incubated overnight. The supernatants were collected and the levels of TNF-α, IL-1β, IL-6, IL-10 and IL-12p70 were measured by ELISA. Data are presented as means ± SEM. $*P < 0.05$; $**P < 0.01$; and $***P < 0.001$ compared to Vehicle.

with the PMAP36-P22 lysozyme fusion protein, P22 lysozyme, and LPS were used as a positive control for the immune response induction (Fig. 6). While P22 lysozyme did not increase the levels of inflammatory cytokines at all, LPS or PMAP36-P22 lysozyme fusion protein markedly increased the immune responses in DCs. These findings demonstrated that the PMAP36-P22 lysozyme fusion protein could affect immune responses independent of P22 lysozyme.

In this study, we successfully expressed and purified the PMAP36-P22 lysozyme fusion protein. In the fusion system, P22 lysozyme serves as a potential fusion partner to enhance the expression level and the solubility of the PMAP36 peptide without the loss of antimicrobial activities and with lower toxicity. Thus, P22 lysozyme when used as a fusion partner could improve the solubility of other AMPs or develop a novel substitute of AMPs.

Note: Supplementary information is available on the Molecules and Cells website (www.molcells.org).

ACKNOWLEDGMENTS

This study was supported by Technology Development Program for Agriculture and Forestry; the Ministry for Food, Agriculture, Forestry, and Fisheries, Republic of Korea (no. 117031-3).

REFERENCES

Bahnsen, J.S., Franzyk, H., Sayers, E.J., Jones, A.T., and Nielsen, H.M. (2015). Cell-penetrating antimicrobial peptides-prospectives for targeting intracellular infections. Pharm. Res. *32*, 1546-1556.

Bulet, P., Dimarcq, J.L., Hetru, C., Lagueux, M., Charlet, M., Hegy, G., Van Dorsselaer, A., and Hoffmann, J.A. (1993). A novel inducible antibacterial peptide of Drosophila carries an O-glycosylated substitution. J. Biol. Chem. *268*, 14893-14897.

Ding, R., Lin, C., Wei, S., Zhang, N., Tang, L., Lin, Y., Chen, Z., Xie, T., Chen, X., Feng, Y., et al. (2017). Therapeutic benefits of mesenchymal stromal cells in a rat model of hemoglobin-induced hypertensive intracerebral hemorrhage. Mol. Cells *40*, 133-142.

Hancock, R.E., and Sahl, H.G. (2006). Antimicrobial and host-defense peptides as new anti-infective therapeutic strategies. Nat. Biotechnol. *24*, 1551-1557.

Huang, Y., Huang, J., and Chen, Y. (2010). Alpha-helical cationic antimicrobial peptides: relationships of structure and function. Protein Cell *1*, 143-152.

Ingham, A.B., and Moore, R.J. (2007). Recombinant production of antimicrobial peptides in heterologous microbial systems. Biotechnol. Appl. Biochem. *47*, 1-9.

Jacoby, T.S., Kuchenbecker, R.S., Dos Santos, R.P., Magedanz, L., Guzatto, P., and Moreira, L.B. (2010). Impact of hospital-wide infection rate, invasive procedures use and antimicrobial consumption on bacterial resistance inside an intensive care unit. J. Hospital Infect. *75*, 23-27.

Li, Y., Xiang, Q., Zhang, Q., Huang, Y., and Su, Z. (2012). Overview on the recent study of antimicrobial peptides: origins, functions, relative mechanisms and application. Peptides *37*, 207-215.

Lv, Y., Wang, J., Gao, H., Wang, Z., Dong, N., Ma, Q., and Shan, A. (2014). Antimicrobial properties and membrane-active mechanism of a potential alpha-helical antimicrobial derived from cathelicidin PMAP-36. PLoS One *9*, e86364.

Lyu, Y., Yang, Y., Lyu, X., Dong, N., and Shan, A. (2016). Antimicrobial activity, improved cell selectivity and mode of action of short PMAP-36-derived peptides against bacteria and Candida. Scientific Reports *6*, 27258.

Mai, X.T., Huang, J., Tan, J., Huang, Y., and Chen, Y. (2015). Effects and mechanisms of the secondary structure on the antimicrobial activity and specificity of antimicrobial peptides. J. Pept. Sci. *21*, 561-568.

Miki, T., and Hardt, W.D. (2013). Outer membrane permeabilization is an essential step in the killing of gram-negative bacteria by the lectin RegIIIbeta. PLoS One *8*, e69901.

Pedulla, M.L., Ford, M.E., Karthikeyan, T., Houtz, J.M., Hendrix, R.W., Hatfull, G.F., Poteete, A.R., Gilcrease, E.B., Winn-Stapley, D.A., and Casjens, S.R. (2003). Corrected sequence of the bacteriophage p22 genome. J. Bacteriol. *185*, 1475-1477.

Rennell, D., and Poteete, A.R. (1989). Genetic analysis of bacteriophage P22 lysozyme structure. Genetics *123*, 431-440.

Scocchi, M., Zelezetsky, I., Benincasa, M., Gennaro, R., Mazzoli, A., and Tossi, A. (2005). Structural aspects and biological properties of the cathelicidin PMAP-36. FEBS J. *272*, 4398-4406.

Storici, P., Scocchi, M., Tossi, A., Gennaro, R., and Zanetti, M. (1994). Chemical synthesis and biological activity of a novel antibacterial peptide deduced from a pig myeloid cDNA. FEBS Lett. *337*, 303-307.

Subbalakshmi, C., Bikshapathy, E., Sitaram, N., and Nagaraj, R. (2000). Antibacterial and hemolytic activities of single tryptophan analogs of indolicidin. Biochem. Biophys. Res. Commun. *274*, 714-716.

Takahashi, D., Shukla, S.K., Prakash, O., and Zhang, G. (2010). Structural determinants of host defense peptides for antimicrobial activity and target cell selectivity. Biochimie *92*, 1236-1241.

Tang, Y.Q., Yuan, J., Osapay, G., Osapay, K., Tran, D., Miller, C.J., Ouellette, A.J., and Selsted, M.E. (1999). A cyclic antimicrobial peptide produced in primate leukocytes by the ligation of two truncated alpha-defensins. Science *286*, 498-502.

Teixeira, V., Feio, M.J., and Bastos, M. (2012). Role of lipids in the interaction of antimicrobial peptides with membranes. Prog. Lipid Res. *51*, 149-177.

van Kan, E.J., Demel, R.A., van der Bent, A., and de Kruijff, B. (2003). The role of the abundant phenylalanines in the mode of action of the antimicrobial peptide clavanin. Biochim. Biophys. Acta *1615*, 84-92.

Wang, G., Li, X., and Wang, Z. (2016). APD3: the antimicrobial peptide database as a tool for research and education. Nucleic Acids Res. *44*, D1087-1093.

Yeaman, M.R., and Yount, N.Y. (2003). Mechanisms of antimicrobial peptide action and resistance. Pharmacol. Rev. *55*, 27-55.

Yeung, A.T., Gellatly, S.L., and Hancock, R.E. (2011). Multifunctional cationic host defence peptides and their clinical applications. Cell Mol. Life Sci. *68*, 2161-2176.

Zasloff, M. (2002). Antimicrobial peptides of multicellular organisms. Nature *415*, 389-395.

Zheng, L., McQuaw, C.M., Ewing, A.G., and Winograd, N. (2007). Sphingomyelin/phosphatidylcholine and cholesterol interactions studied by imaging mass spectrometry. J. Am. Chem. Soc. *129*, 15730-15731.